Earth and Planetary Science Letters 545 (2020) 116400

Contents lists available at ScienceDirect

Earth and Planetary Science Letters

www.elsevier.com/locate/epsl

Ferromagnetic resonance of magnetite biominerals traces redox changes

Thomas M. Blattmann [a,b,*], Barbara Lesniak [c], Inés García-Rubio [d,e], Michalis Charilaou [f], Martin Wessels [g], Timothy I. Eglinton [b], Andreas U. Gehring [c,**]

[a] Biogeochemistry Research Center, JAMSTEC, 237-0061 Yokosuka, Japan
[b] Geological Institute, ETH Zurich, 8092 Zurich, Switzerland
[c] Institute of Geophysics, ETH Zurich, 8092 Zurich, Switzerland
[d] Laboratory of Physical Chemistry, ETH Zurich, 8093 Zurich, Switzerland
[e] Centro Universitario de la Defensa, 50090 Zaragoza, Spain
[f] Department of Physics, University of Louisiana at Lafayette, Lafayette, LA 70504, USA
[g] Institut für Seenforschung, Landesanstalt für Umwelt Baden-Württemberg, 88085 Langenargen, Germany

ARTICLE INFO

Article history:
Received 18 October 2019
Received in revised form 12 May 2020
Accepted 5 June 2020
Available online 16 June 2020
Editor: I. Halevy

Keywords:
magnetotactic bacteria
magnetofossil
anoxia
sediment
redox gradient
eutrophication

ABSTRACT

Redox variations govern a multitude of key geochemical and microbiological processes within lacustrine and marine systems, yet the interpretation of these geological archives can be limited because redox-sensitive microorganisms leave behind sparse fossil evidence. Here, we assess a biologically controlled magnetic proxy through investigation of a well-constrained sedimentary record covering a perturbation of redox-conditions driven by a complete trophic cycle in Lake Constance. Ferromagnetic resonance spectroscopy of sediments reveals strong uniaxial anisotropy, indicative of single-domain magnetite particles in intact or fragmentary chain arrangements, which are an unambiguous trait of magnetotactic bacteria (MTB) and their magnetofossil remains. We show that biogenic magnetite formed intra-cellularly in MTB faithfully records changing redox-conditions at or close to the sediment water-interface. Biogenic magnetite within sedimentary records points to the proliferation of MTB parallel to a decline in water column dissolved oxygen and the formation of sulfidic surface sediments in Lake Constance associated with an episode of eutrophication (1955–1991). We conclude that magnetofossils may serve as a sensitive geological proxy to reconstruct dynamic redox-changes along the sediment-water interface and bottom waters.

1. Introduction

Understanding the impact of redox dynamics within aquatic systems is important for reconstructing biogeochemical processes in marine and lacustrine sedimentary records. Changing redox conditions can drive faunal changes, which in turn critically affect fossil assemblages and molecular (biomarker) signatures preserved in the geological record (Gambacorta et al., 2016). Redox-sensitive microorganisms such as magnetotactic bacteria (MTB), which are present in freshwater and marine settings, are of special interest because they may play an appreciable role in the cycling of iron in aquatic systems (Chen et al., 2014) and can leave evidence of their existence in sediments in the form of magnetofossils (Hesse, 1994; Kind et al., 2012; Kodama et al., 2013; Kopp and Kirschvink, 2008; Roberts et al., 2012). These intracellularly produced ferrimagnetic nanoparticles, generally composed of magnetite ($Fe^{2+}Fe_2^{3+}O_4$), denoted magnetosomes, are characterized by genetically-determined, well-defined sizes (typically 35-120 nm) with narrow shape distributions in the single-domain (SD) magnetic state (Bazylinski et al., 1988; Devouard et al., 1998). Magnetosomes are aligned in chains along a cytoskeletal filament that stabilizes their arrangement and prevents clumping (Kopp et al., 2006; Scheffel et al., 2006). This linear arrangement generates a magnetic dipole that is used by MTB as a compass to navigate along Earth's magnetic field (i.e., magnetotaxis) toward favored habitats around the oxic-anoxic transition zone (OATZ) (e.g., Spormann and Wolfe, 1984). MTB and their remains have been reported from Quaternary deposits (Kind et al., 2012; Kodama et al., 2013), but magnetofossil evidence extends back to the Cretaceous (Kopp and Kirschvink, 2008), with genes associated with magnetosome formation originating in the

* Corresponding author at: Biogeochemistry Research Center, JAMSTEC, 237-0061 Yokosuka, Japan.
** Corresponding author.
E-mail addresses: blattmannt@jamstec.go.jp (T.M. Blattmann), agehring@ethz.ch (A.U. Gehring).

https://doi.org/10.1016/j.epsl.2020.116400
0012-821X/

Archean (Lin et al., 2017). Paleomagnetic studies are increasingly considering and seeking to extract paleoenvironmental information (e.g., nutrient availability, dissolved iron availability, oxygen concentrations) from magnetofossils embedded within a complex matrix of magnetic minerals in sedimentary records (Larrasoaña et al., 2003; Passier et al., 2001; Roberts et al., 2011, 2012; Savian et al., 2014; Suk, 2016). Given the OATZ habitat of MTB and the stability of magnetosomes, magnetofossils may serve as ideal redox-sensitive proxies in geological archives as postulated previously (Chang et al., 2018; Hawthorne and McKenzie, 1993; Larrasoaña et al., 2014). In recent years, ferromagnetic resonance (FMR) spectroscopy has been established as a powerful tool to quantitatively analyze the magnetic traits of cultured MTB (Charilaou, 2017; Kopp et al., 2006), and this in turn opened the door to detect MTB and magnetofossils in geological samples (Gehring et al., 2011a). Moreover, the FMR spectral response allows the essential discrimination between biogenic and detrital magnetite characterized by SD and multi-domain, respectively (e.g., Gehring et al., 2009; Griscom, 1980), paving the way for magnetofossil identification in sedimentary records and extracting environmental changes.

Here, we present the FMR spectral evolution yielded from a historically chronicled redox perturbation recorded in a sediment core from Lake Constance spanning the mid-19th to early 21st Century as a testbed to decipher the response of MTB. The rise and fall of MTB as witnessed by their magnetofossil legacy in sediments is proposed as a proxy for past water column and sediment-water interface redox changes.

2. Materials and methods

2.1. Study site and sampling

Lake Constance, bordering Switzerland, Austria, and Germany, is the second largest peri-alpine lake in Central Europe and includes a shelf, margin, and abyssal plain similar to ocean basin bathymetry (IGKB, 2016; Müller, 1966b; Wessels, 1998a). The study site (47.5997°N 9.3581°E) on the southern slope of the lake at a water depth of 100 m and sedimentation rate of 1-2 mm/y, is a reference locality for monitoring of lacustrine primary productivity (Blattmann et al., 2019; Fuentes et al., 2013; IGKB, 2009; Wessels et al., 1999) and is representative of environmental changes since the Late Glacial period (Wessels, 1998b). For this study, a ~1 m gravity core (BO12-111) was retrieved in December 2012, extruded, split in sections based on color (Fig. 1) and transferred to polyethylene bags. Each sample was homogenized, frozen at −20 °C, and freeze-dried prior to analysis.

2.2. Sedimentary sulfur and organic carbon

Carbon and sulfur contents were determined using an elemental analyzer (including an acidification module and furnace) coupled to an infrared detector (Analytik Jena multiEA 4000). Total inorganic carbon content was quantified using an acidification module by applying 15-20% orthophosphoric acid onto the sample material under gentle heating and measuring evolved CO_2 until the reaction was complete. Total carbon and sulfur were measured by combustion at 1450 °C under O_2 flow. The instrument was calibrated using calcium carbonate and calcium sulfate dihydrate standards for carbon and sulfur, respectively. Total organic carbon (TOC) was determined by difference between total carbon and total inorganic carbon.

2.3. Ferromagnetic resonance spectroscopy

FMR spectroscopy is used for the characterization of magnetic materials, specifically for the measurement of the magnetocrystalline and the uniaxial magnetic anisotropy fields (e.g., Vonsovskii, 1966). In recent years, it has been successfully applied to quantitatively analyze the magnetic properties of cultured MTB (Charilaou et al., 2011a, 2015) and to detect magnetofossils in sedimentary deposits (Gehring et al., 2011a; Kind et al., 2012; Kopp et al., 2006; Roberts et al., 2011). In the following, we summarize the basic FMR principles to justify the concept of spectral analysis in our study. In an FMR experiment, the sample is subjected to a DC external magnetic field and an orthogonal microwave field. The DC field drives the magnetic moment of the sample to a precession around the field axis at a frequency that increases linearly with the strength of the external field, i.e., the Larmor frequency, $\omega_L = g\mu_B B_{\text{eff}}/\hbar$, where $\hbar$ is the reduced Planck constant, g is the Landé spectroscopic splitting factor, μ_B is the Bohr magneton, and B_{eff} is the effective magnetic field in the sample, consisting of both internal (exchange and anisotropy) and external fields (DC field and microwave field). Once the precession frequency matches that of the incident microwave radiation, i.e., $\omega_L = \omega_{mw}$, resonance occurs and the sample absorbs microwave radiation as the magnetic moments precess at maximum amplitude. In a FMR spectrum, the resonance event is recorded as the absorption of microwaves that results in a resonance field, as a function of the external magnetic field. When the resonance condition is fulfilled, the absorption exhibits a maximum, and the FMR spectrum for a simple isotropic system has the shape of a distribution function, e.g., a Lorentzian or a Gaussian profile, centered at a resonance field denoted B_{eff}. Fig. 2A shows a FMR spectrum of an isotopic system with $g = 2.05$. In a system with magnetic anisotropy, i.e., SD magnetite particles and chain assemblies, there is an easy axis and a hard axis. The FMR spectrum is shifted along the field axis depending on the uniaxial internal field. When measured along the easy axis, the resonance field will be lower than that of the isotropic system, and when the measurement is along the hard axis the resonance field will be higher than that of the isotropic system (Fig. 2B). Hence, with FMR spectroscopy, we obtain quantitative information about the internal fields of the sample.

In contrast to the spectra of oriented magnetic dipoles like those shown in Fig. 2B (Charilaou et al., 2014), magnetosomes

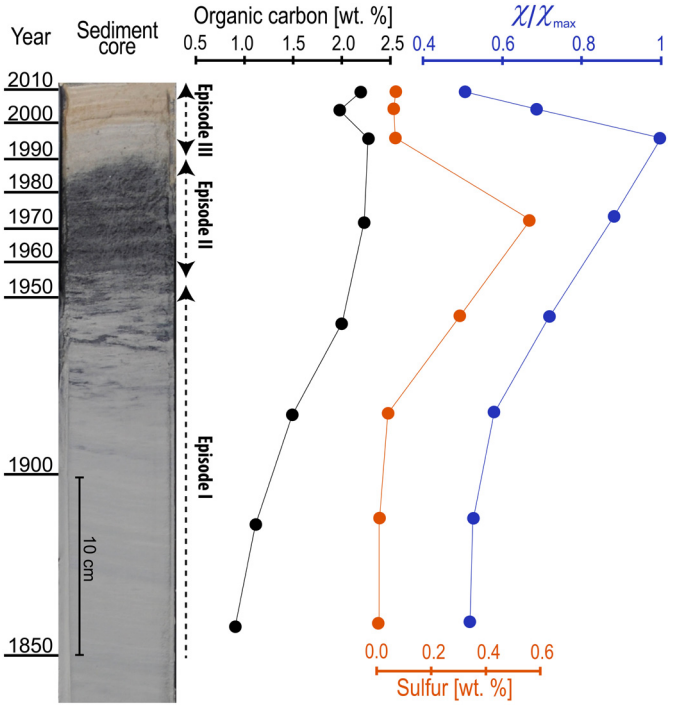

Fig. 1. Lake Constance sediment profile with chronology, organic carbon content, total sulfur content, and normalized magnetic susceptibility.

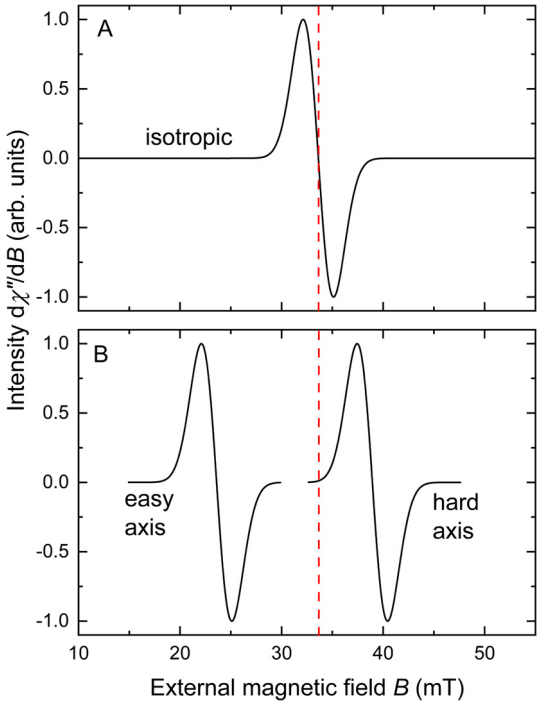

Fig. 2. First derivative absorption FMR spectra of (A) an isotropic system with $g = 2.05$ and (B) of a uniaxial system along its easy and hard axis. The vertical dashed line shows the resonance field of the isotropic system. The anisotropy shifts the spectra along the field axis, i.e., to lower field for the easy axis and to higher fields for the hard axis. Along the easy axis, the anisotropy field is parallel to the external field and contributes to the precession, and therefore a smaller external field is needed to achieve resonance. Contrarily, along the hard axis, the external field needs to compensate for the anisotropy field, which is off-axis to the external field.

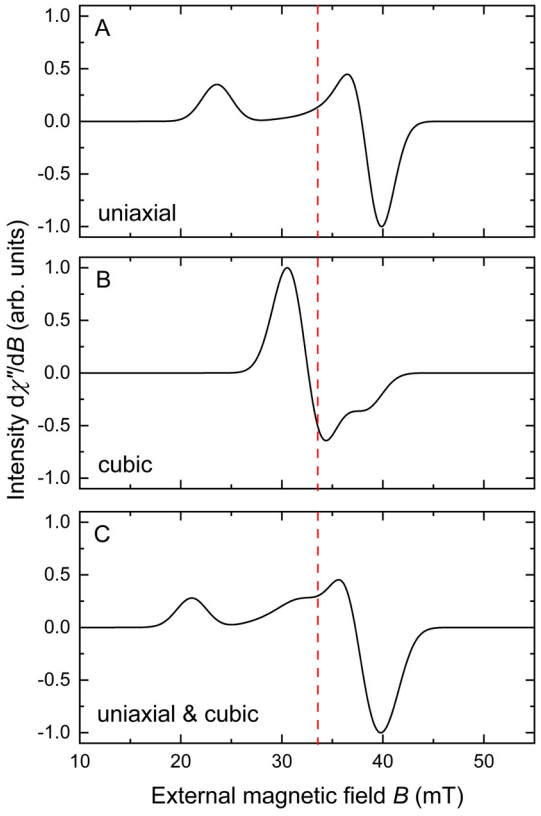

Fig. 3. Convoluted FMR spectra of (A) a purely uniaxial system, (B) a purely cubic system, and (C) a combined uniaxial and cubic system, corresponding to the spectrum of an ensemble of MTB.

chains are generally randomly distributed within sediments, and therefore all resonance events are recorded at once and convoluted in the spectrum. A statistical treatment of the FMR, as described by Charilaou et al. (2011a), quantifies the components of the FMR spectrum and determines the magnetic properties of chains. Figs. 3A and 3B show the convoluted FMR spectrum of a uniaxial and a cubic system, respectively. The spectra are spread around the isotropic resonance field and their shapes are due to the distribution of resonance fields in the sample. In MTB, the FMR spectrum in Fig. 3C is a convolution of resonance fields combining both uniaxial and cubic symmetries. This spectrum corresponds to a system with MTB that have exactly the same magnetic properties, i.e., uniaxial anisotropy field (B_{uni}) and cubic anisotropy field (B_{cub}). In sedimentary samples that consist of multiple MTB species with different corresponding magnetofossils in varying states of preservation, the spectral response becomes more complex.

In this study, the FMR spectra of the sediment samples were recorded on a X-band Bruker E500 EPR spectrometer working at a frequency of 9.81 GHz, 0.06 mW power, 0.1 mT modulation amplitude, and a modulation frequency of 100 kHz. The spectra were simulated with the algorithm by Charilaou et al. (2011a). Using FMR spectra, contributions from paramagnetic species (mostly Mn^{2+}) are quantified and prior to spectral simulation, the paramagnetic signal at $g \approx 2$ was removed as proposed by Maloof et al. (2007). The FMR spectroscopy was complemented by mass magnetic susceptibility (χ) measurements on an AGICO MFK1 Kappabridge and by first order reversal curve (FORC) analysis (Pike et al., 1999) of the sample with the highest χ using a MicroMag 3900 vibrating sample magnetometer and the FORClab code for the data processing (Winklhofer and Zimanyi, 2006).

3. Results and discussion

3.1. Sediment description and chronology

Depth intervals from the uppermost 32 cm of the gravity core were investigated, which encompasses the last 160 years and spans a complete cycle of eutrophication and re-oligotrophication (Müller, 1997). The chronology of these sediments is subdivided into three episodes (Fig. 1), with deposition ages constrained by the present-day sedimentation rate of 1.9 mm/yr (Blattmann et al., 2019). Episode I (1850-1955 AD), corresponding to 21 cm of deposition, is characterized by monotonous bluish-gray clayey silt with dark striations representing a shoaling of the oxidation front upon continued burial (Hummel, 1923). Sediments darken continuously upward in the core toward episode II, which reflects encroaching eutrophic conditions due to increasing anthropogenic phosphorous inputs into the lake (Müller, 1997; Wessels et al., 1999). In episode II (1955-1991 AD), dark sediment with a pungent sulfidic odor marks the deposition of iron sulfide-bearing sediments during the most eutrophic stage (Müller, 1966a, 1966b; Wagner, 1971). These sulfidic, dark clayey silts abruptly transition toward the core top into bluish-gray finely laminated and fluffy light brown clayey silts of episode III (1991-2012 AD). The brownish hue of the most recent deposits (uppermost 2 cm) is indicative of a ferric phase and points to oxic conditions. Hummel (1923) also described such a hue for sediments that are now bluish-gray.

3.2. Biogeochemistry of sediments and water column

Extensive water column and surface sediment monitoring of Lake Constance over the past century offers a real-time geological window to link sedimentary total organic carbon (TOC) and total

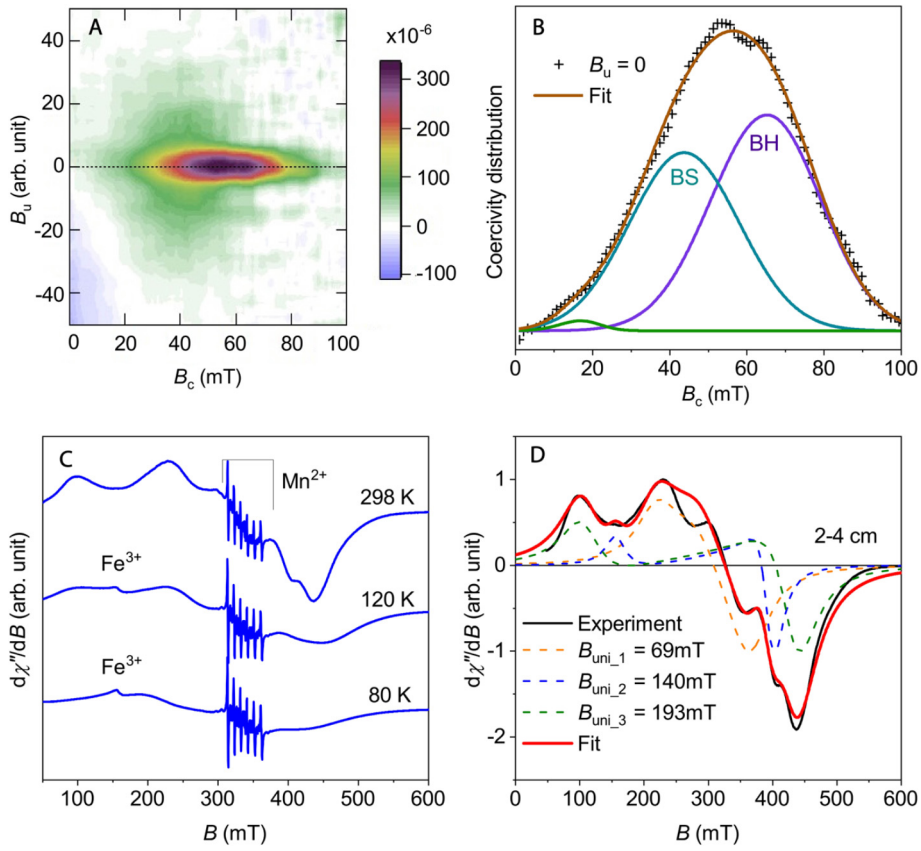

Fig. 4. FORC curve of the sample with the highest χ (A), deconvolution of B_c profile along $B_u = 0$ with the two major Gaussian components denoted B(S) and B(H) and a minor one (B), corresponding FMR spectra superimposed by a Mn^{2+} signal at room and low-temperature (C), simulation of the experimental FMR spectrum obtained from the sample at room temperature as superposition of three components with different uniaxial fields (dashed lines) using the model of Charilaou et al. (2011a), the Mn^{2+} is omitted for clarity (D) (For interpretation of the colors in the figure(s), the reader is referred to the web version of this article.)

sulfur (TS) contents. In our profile (Fig. 1), TOC content ranges between 0.8 and 2.4 wt% and generally increases toward the present. The TS content varies between 0.01 and 0.6 wt%. In the later part of episode I, TS increases to a maximum in episode II. Such change is indicative of a shift from oxic or post-oxic to prevailing anoxic conditions (Berner, 1981). For the TOC content, the effect of eutrophication is obscured due to early diagenetic processes that resulted in the attenuation of organic matter degradation during burial (Blattmann et al., 2019; Müller, 1997). Beginning in the mid-19th Century, the TS trend and historical accounts (Hoppe-Seyler, 1895) are consistent with an absence of sulfides, and that massive sulfide formation began in the 1950s (Lehn, 1976; Wagner, 1971). Moreover, increased TS correlates with the overall nutrient state of Lake Constance. The latter is gauged by water column dissolved phosphorous content that peaked in 1979 (Müller, 1997; Wessels et al., 1999), manifesting itself in the sulfidic sediments of episode II. During peak eutrophication, algal biomass increased approximately five-fold (Kümmerlin, 1998). This is consistent with observed dissolved oxygen contents in deep waters (which began in the 1890s) that reveal increasingly frequent and intense late-summer decreases into the 1950s due to enhanced settling and decay of organic matter (Elster and Einsele, 1937; Grim, 1955; Hoppe-Seyler, 1895; Lehn, 1976; Muckle, 1967; Rhodes et al., 2017; Wagner and Kruse, 1995). Oxygen replenishment in deep waters is driven by seasonal water column mixing and the influx of subducted riverine water masses, especially from the Alpine Rhine (Fink et al., 2016; Rhodes et al., 2017) and from littoral areas and bays. Compared to the 6.5 to 10 mm oxygen penetration depth into the sediment during the oligotrophic state (IGKB, 2009; Melton et al., 2014; Rahalkar et al., 2009), heightened organic matter burial and oxygen consumption by remineralization led to shoaling of the OATZ with reported oxygen penetration depths of <2 mm, virtually reaching the sediment-water interface (Frenzel et al., 1990; Müller, 1966a; Wagner, 1967). In concert with eutrophication, bacterial biomass increased approximately tenfold and has contributed critically to dissolved oxygen consumption (Deufel, 1967, 1972). MTB are reported from other anthropogenically perturbed perialpine lakes, such as the lakes Chiemsee, Greifensee or Soppensee (e.g., Hawthorne and McKenzie, 1993; Spring et al., 2000; Kind et al., 2012), raising the possibility of their presence in Lake Constance.

3.3. Sediment magnetic properties

The magnetic susceptibility χ varies between 9.44 and 18.87 $\times$ 10^{-8} SI with a relative maximum ($\chi/\chi_{max} = 1$) at the earliest part of episode III coinciding with re-oligotrophication and re-establishment of pre-eutrophic oxygenated conditions in the water column (Fig. 1). Such an enhanced χ has been observed in several locations throughout the lake (Wessels, 1995). During episode III, χ declines continuously and reassumes pre-eutrophic levels (Fig. 1). The variation in χ is also mirrored in the FMR response, i.e. the strongest signal due to the highest ferromagnetic content corresponds with the highest, relative χ (i.e., with $\chi/\chi_{max} = 1$).

The FMR spectrum at room temperature obtained from the layer with $\chi/\chi_{max} = 1$ (Fig. 4D) revealed broad ferrimagnetic features upon which a six-line signal typical for structure-bound Mn^{2+} in carbonates is superimposed (Fig. 4C). The low-temperature behavior of FMR spectra shows characteristic broadening associated with the Verwey transition diagnostic for magnetite,

and indicates negligible contributions of greigite (Fe_3S_4) as another possible ferrimagnetic phase in MTB since the latter does not feature a magnetic transition at low temperatures (Chen et al., 2014; Gehring et al., 2011b). Using the method of Charilaou et al. (2011a), the relatively complex FMR spectrum can be simulated with the magnetocrystalline anisotropy field $B_{cub} = -23.5$ mT for magnetite at room temperature and multiple uniaxial field B_{uni} components (Fig. 4D). The strongest uniaxial anisotropy with $B_{uni} = 193$ mT is similar to that of a wild-type MTB with multiple magnetosome chains (Abraçado et al., 2014). The slightly lower B_{uni} =140 mT is comparable to values for single chains of laboratory-cultured MTB species (Charilaou et al., 2011b; Ghaisari et al., 2017). Given this, the two spectral components can be attributed to intact magnetosome chains. The origin of the third one ($B_{uni} \approx 60$ mT) is less specific, but could be due to disintegrated chains that vary from chain fragments to SD magnetite particles (Charilaou et al., 2011a, 2011b; Faivre et al., 2010). The detection of MTB by the pronounced B_{uni} is supported by a central ridge of the coercivity (B_c) in the FORC diagram (Fig. 4A) that is a diagnostic feature for magnetic particle arrangements found in MTB (Egli et al., 2010; Roberts et al., 2012). Following Egli (2004), the central ridge can be deconvoluted into a bacterial soft (BS) component with 40-45 mT modal coercivity, a bacterial hard (BH) component 60-70 mT (Fig. 4B). A third minor component stems most likely from isolated magnetosomes (Fischer et al., 2008). Independent of microscopic evidence (e.g., Snowball, 1994; Chen et al., 2014), the high magnetic anisotropy obtained from FMR and the FORC data provides clear evidence for a chain arrangement of SD magnetite formed by MTB (e.g., Egli, 2004; Fischer et al., 2008; Faivre et al., 2010; Charilaou et al., 2011b).

Superimposed upon the FMR spectra throughout the profile are also Mn^{2+} signals and for the weaker spectra obtained from samples at >15 cm depth, a Fe^{3+} signal most likely associated with clay minerals becomes relatively pronounced (Meads and Malden, 1975). The FMR simulation after removal of the Mn^{2+} signal reveals that the spectra from episodes II and III have superimposed signals with high B_{uni} that are characteristic of intact magnetosome chains and of signals with $B_{uni} < 100$ mT that are attributed to chain fragments and/or isolated magnetite particles (Fig. 4D, 5, and S1). In the latter case, the spectral contribution with $B_{uni} = 0$ mT can be attributed either to isolated, superparamagnetic or SD magnetite particles with nearly equidimensional shapes that were most likely formed by MTB species such as *Magnetospirillum gryphiswaldense* (Scheffel et al., 2006). The deconvoluted FMR spectra of the top of episode I (11-15 cm) also reveal a mixture of magnetite in chains with $B_{uni} = 178$ mT and SD magnetite particles with no specific arrangement, i.e. $B_{uni} < 100$ mT (Fig. 5 and S1). In contrast, there is no spectral evidence for magnetite in chains in the lower part of episode I (Fig. 5).

In a MTB growth experiment, it has been shown that the shape of a FMR spectrum continuously changes during the formation of the magnetosome chains (Faivre et al., 2010) and that this formation can quantitatively be described by means of B_{uni} (Charilaou et al., 2011b). With this in mind the decrease in B_{uni} can then be taken to infer the reverse process, i.e., the breakdown of magnetite chains in a natural environment, as documented in the sediment record (Fig. 5; S1).

3.4. Productivity and preservation of magnetofossils

Iron in mixed valence states is needed to form magnetite and it has previously been suggested that the iron activity within a depositional environment is a critical factor in MTB growth (Roberts et al., 2011). In Lake Constance, high organic matter fluxes to the sediment floor in the course of eutrophication leads to the shoaling of the OATZ toward the sediment-water interface and elevates the

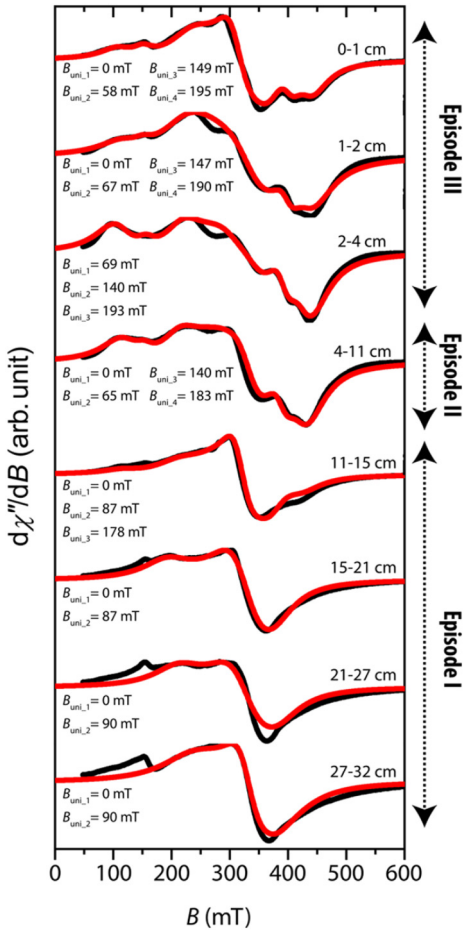

Fig. 5. FMR spectra of the sediment core at room temperature and their simulation with $B_{cub} = -235$ mT for magnetite.

dissolved iron concentrations released to the lower water column (Müller, 1997; Roßknecht, 1998). In our profile, such conditions are indicated by the simultaneous increase in TOC and content of SD magnetic particles throughout episode II (Fig. 1). The sediments of this episode are characterized by the high relative content of magnetite as indicated by χ/χ_{max}, and by uniaxial anisotropy fields that suggest different arrangements of the ferrimagnetic particles, and this in turn points to variable preservation states of the magnetofossils between chains and dispersed magnetosomes (Fig. 5). The historically chronicled zenith in eutrophication with a peak in dissolved phosphorous in 1979 (Müller, 1997) precedes the maximum in relative χ, i.e., the peak in MTB productivity (Fig. 1). This maximum occurs at the onset of re-oligotrophication, which is characterized by a sharp redox gradient near the sediment-water interface with sulfidic deposits and well-oxygenated waters only millimeters apart (transition from episode II to III). Such an environment is ideal for the growth of microaerophilic MTB (e.g., Scheffel et al., 2006). Moreover, the maximum in MTB production, indicated by high χ/χ_{max}, goes along with a high degree of the preservation of magnetosomes in chains as inferred from the FMR spectra (Figs. 1 and 5). Over the course of re-oligotrophication, a downwards retreat of the OATZ, away from the sediment-water interface, leads to a decrease in magnetosome content indicated by a decrease of χ/χ_{max} to a level similar to that yielded from the sediments deposited before the maximum eutrophication during episode II. Therefore, the highest abundance of magnetofossils coincides with re-oxygenation, which is also similarly recorded in a marine environment case study (Passier et al., 2001).

The above link between magnetic and environmental information provides insight into the production and preservation of MTB in sedimentary deposits. The comparison of FMR spectra obtained from the Lake Constance sediment profile shows that magnetofossils, i.e., chain fragments and clumped or dispersed SD magnetite particles, are preserved. This relatively short diagenetic history of less than 150 years illustrates that the preservation of intact MTB chains in geological systems is limited. Nevertheless, the preservation of the magnetosomes can be used to constrain MTB productivity provided the magnetosomes are not affected by dissolution or mixing in the sediments with detrital magnetite. In our profile, these general conditions are met by the course of the magnetite content over time and the absence of multi-domain magnetic particles. With this in mind, our sediment core clearly indicates that the variations in magnetosome abundance, i.e. MTB productivity, records redox-changes in a depositional environment.

4. Conclusions

Quantitative FMR spectroscopy of a sediment core recording a trophic cycle in Lake Constance shows that the magnetic content consists of SD magnetite particles originating from MTB, where they were formed as intracellular chains. The intact magnetosome chains break apart during diagenesis and are preserved as magnetofossils. Decadal-scale variations in magnetofossil content reflect MTB activity during the trophic cycle. With the return of an oligotrophic state, the redox gradient along the sediment-water interface steepened owing to replenishing deep-water oxygen diffusing into near-surface sulfidic sediments. Capitalizing on this redox gradient, MTB thrive. Under establishment of these oligotrophic conditions and upon continued sedimentary burial, the OATZ horizon deepened, leading to the rapid demise of the MTB. This, in turn, leads to the sedimentary magnetic properties reassuming pre-perturbation, background characteristics. With this in mind, preserved magnetosome assemblies and their concentration as inferred from FMR spectra in combination with χ/χ_{max} can shed light on past microbiological activity in response to redox-changes in a depositional environment. Finally, MTB and their fossil remains are ideal carriers of paleomagnetic information, and therefore, in a magnetostratigraphic context, magnetofossils have great potential to constrain time-resolved microbiological response to redox-changes in geological systems.

Declaration of competing interest

The authors declare that they have no known competing financial interests or personal relationships that could have appeared to influence the work reported in this paper.

Acknowledgements

The authors thank Dimitrios Koulialias, Andrew Roberts, and anonymous reviewers for their critical comments on the manuscript and Michael Plötze (ClayLab ETH Zürich) for providing laboratory support for elemental analysis. The project was supported by Swiss National Sciences Foundation grant no. 200021_165851 and ETH research grant ETH-41 14-1. T.M. Blattmann acknowledges funding from JAMSTEC and JSPS KAKENHI Grant (19K23475) and I. García-Rubio acknowledges funding from grants MINECO (CTQ2015-64486-R) and Gobierno de Aragón (E35_17R) and Fondo Social Europeo-"*Construyendo Europa desde Aragón*".

Appendix A. Supplementary material

Supplementary material related to this article can be found online at https://doi.org/10.1016/j.epsl.2020.116400.

References

Abraçado, L.G., Wajnberg, E., Motta, D., Keim, C.N., Silva, K., Moreira, E.T., Lins, U., Farina, M., 2014. Ferromagnetic resonance of intact cells and isolated crystals from cultured and uncultured magnetite-producing magnetotactic bacteria. Phys. Biol. 11 (3), 036006.

Bazylinski, D.A., Frankel, R.B., Jannasch, H.W., 1988. Anaerobic magnetite production by a marine, magnetotactic bacterium. Nature 334 (6182), 518–519.

Berner, R.A., 1981. A new geochemical classification of sedimentary environments. J. Sediment. Res. 51 (2), 359–365.

Blattmann, T.M., Wessels, M., McIntyre, C.P., Eglinton, T.I., 2019. Petrogenic organic carbon retention in terrestrial basins: a case study from perialpine Lake Constance. Chem. Geol. 503, 52–60.

Chang, L., Harrison, R.J., Zeng, F., Berndt, T.A., Roberts, A.P., Heslop, D., Zhao, X., 2018. Coupled microbial bloom and oxygenation decline recorded by magnetofossils during the Palaeocene–Eocene Thermal Maximum. Nat. Commun. 9 (1), 4007.

Charilaou, M., 2017. Ferromagnetic resonance of biogenic nanoparticle-chains. J. Appl. Phys. 122 (6), 063903.

Charilaou, M., Winklhofer, M., Gehring, A.U., 2011a. Simulation of ferromagnetic resonance spectra of linear chains of magnetite nanocrystals. J. Appl. Phys. 109 (9), 093903.

Charilaou, M., Sahu, K.K., Faivre, D., Fischer, A., García-Rubio, I., Gehring, A.U., 2011b. Evolution of magnetic anisotropy and thermal stability during nanocrystal-chain growth. Appl. Phys. Lett. 99 (18), 182504.

Charilaou, M., Kind, J., García-Rubio, I., Schüler, D., Gehring, A.U., 2014. Magnetic anisotropy of non-interacting collinear nanocrystal-chains. Appl. Phys. Lett. 104 (11), 112406.

Charilaou, M., Rahn-Lee, L., Kind, J., García-Rubio, I., Komeili, A., Gehring, A.U., 2015. Anisotropy of bullet-shaped magnetite nanoparticles in the magnetotactic bacteria *Desulfovibrio magneticus sp.* strain RS-1. Biophys. J. 108 (5), 1268–1274.

Chen, A.P., Berounsky, V.M., Chan, M.K., Blackford, M.G., Cady, C., Moskowitz, B.M., Kraal, P., Lima, E.A., Kopp, R.E., Lumpkin, G.R., Weiss, B.P., Hesse, P., Vella, N.G.F., 2014. Magnetic properties of uncultivated magnetotactic bacteria and their contribution to a stratified estuary iron cycle. Nat. Commun. 5, 4797.

Deufel, J., 1967. Hydrobakteriologische Untersuchungen im Bodensee I. Über die Vertikalverteilung der Bakterien im Pelagial. Int. Rev. Gesamten Hydrobiol. Hydrograph. 52 (4), 617–626.

Deufel, J., 1972. Hydrobakteriologische Untersuchungen im Bodensee III. Progressive Zunahme der planktonabhängigen Bakterienproduktion als Zeichen der Eutrophierung. Int. Rev. Gesamten Hydrobiol. Hydrograph. 57 (1), 153–156.

Devouard, B., Pósfai, M., Hua, X., Bazylinski, D.A., Frankel, R.B., Buseck, P.R., 1998. Magnetite from magnetotactic bacteria: size distributions and twinning. Am. Mineral. 83, 1387.

Egli, R., 2004. Characterization of individual rock magnetic components by analysis of remanence curves. 3. Bacterial magnetite and natural processes in lakes. Phys. Chem. Earth Parts A/B/C 29 (13), 869–884.

Egli, R., Chen, A.P., Winklhofer, M., Kodama, K.P., Horng, C.-S., 2010. Detection of noninteracting single domain particles using first-order reversal curve diagrams. Geochem. Geophys. Geosyst. 11.

Elster, H.-J., Einsele, W., 1937. Beiträge zur Hydrographie des Bodensees [Obersee]. Int. Rev. Gesamten Hydrobiol. Hydrograph. 35 (1–6), 522–585.

Faivre, D., Fischer, A., Garcia-Rubio, I., Mastrogiacomo, G., Gehring, A.U., 2010. Development of cellular magnetic dipoles in magnetotactic bacteria. Biophys. J. 99 (4), 1268–1273.

Fink, G., Wessels, M., Wüest, A., 2016. Flood frequency matters: why climate change degrades deep-water quality of peri-Alpine lakes. J. Hydrol. 540, 457–468.

Fischer, H., Mastrogiacomo, G., Löffler, J.F., Warthmann, R.J., Weidler, P.G., Gehring, A.U., 2008. Ferromagnetic resonance and magnetic characteristics of intact magnetosome chains in *Magnetospirillum gryphiswaldense*. Earth Planet. Sci. Lett. 270 (3), 200–208.

Frenzel, P., Thebrath, B., Conrad, R., 1990. Oxidation of methane in the oxic surface layer of a deep lake sediment (Lake Constance). FEMS Microbiol. Lett. 73 (2), 149–158.

Fuentes, N., Güde, H., Wessels, M., Straile, D., 2013. Allochthonous contribution to seasonal and spatial variability of organic matter sedimentation in a deep oligotrophic lake (Lake Constance). Limnologica 43 (2), 122–130.

Gambacorta, G., Bersezio, R., Weissert, H., Erba, E., 2016. Onset and demise of Cretaceous oceanic anoxic events: the coupling of surface and bottom oceanic processes in two pelagic basins of the western Tethys. Paleoceanography 31 (6), 732–757.

Gehring, A.U., Fischer, H., Louvel, M., Kunze, K., Weidler, P.G., 2009. High temperature stability of natural maghemite: a magnetic and spectroscopic study. Geophys. J. Int. 179 (3), 1361–1371.

Gehring, A.U., Kind, J., Charilaou, M., García-Rubio, I., 2011a. The detection of magnetotactic bacteria and magnetofossils by means of magnetic anisotropy. Earth Planet. Sci. Lett. 309 (1), 113–117.

Gehring, A.U., Fischer, H., Charilaou, M., García-Rubio, I., 2011b. Magnetic anisotropy and Verwey transition of magnetosome chains in *Magnetospirillum gryphiswaldense*. Geophys. J. Int. 187 (3), 1215–1221.

Ghaisari, S., Winklhofer, M., Strauch, P., Klumpp, S., Faivre, D., 2017. Magnetosome organization in magnetotactic bacteria unraveled by ferromagnetic resonance spectroscopy. Biophys. J. 113 (3), 637–644.
Grim, J., 1955. Die chemischen und planktologischen Veränderungen des Bodensee-Obersees in den letzten 30 Jahren. Arch. Hydrobiol. 22 (3–4), 310–322.
Griscom, D.L., 1980. Ferromagnetic resonance of fine grained precipitates in glass: a thumbnail review. J. Non-Cryst. Solids 42 (1), 287–296.
Hawthorne, T.B., McKenzie, J.A., 1993. Biogenic magnetite: authigenesis and diagenesis with changing redox conditions in Lake Greifen, Switzerland. In: Aïssaoui, D.M., McNeill, D.F., Hurley, N.F. (Eds.), Applications of Paleomagnetism to Sedimentary Geology, vol. 49. SEPM.
Hesse, P.P., 1994. Evidence for bacterial palaeoecological origin of mineral magnetic cycles in oxic and sub-oxic Tasman Sea sediments. Mar. Geol. 117 (1), 1–17.
Hoppe-Seyler, F., 1895. Über die Verteilung absorbierter Gase im Wasser des Bodensees und ihre Beziehung zu den in ihm lebenden Tieren und Pflanzen. Schr. Ver. Gesch. Bodensees Umgeb. 24, 29–48.
Hummel, K., 1923. Über Sedimentbildung im Bodensee: Geologisches Archiv von Ernst Kraus. Z. Gesamte Geol. Deren Nachbargeb. 2, 35–45.
IGKB, 2009. Bodensee-Untersuchung-Seeboden, vol. 56, p. 107.
IGKB, 2016. Tiefenschärfe – Hochauflösende Vermessung des Bodensees, vol. 61, p. 109.
Kind, J., van Raden, U.J., García-Rubio, I., Gehring, A.U., 2012. Rock magnetic techniques complemented by ferromagnetic resonance spectroscopy to analyse a sediment record. Geophys. J. Int. 191 (1), 51–63.
Kodama, K.P., Moeller, R.E., Bazylinski, D.A., Kopp, R.E., Chen, A.P., 2013. The mineral magnetic record of magnetofossils in recent lake sediments of Lake Ely, PA. Glob. Planet. Change 110, 350–363.
Kopp, R.E., Kirschvink, J.L., 2008. The identification and biogeochemical interpretation of fossil magnetotactic bacteria. Earth-Sci. Rev. 86 (1), 42–61.
Kopp, R.E., Weiss, B.P., Maloof, A.C., Vali, H., Nash, C.Z., Kirschvink, J.L., 2006. Chains, clumps, and strings: magnetofossil taphonomy with ferromagnetic resonance spectroscopy. Earth Planet. Sci. Lett. 247 (1), 10–25.
Kümmerlin, R.E., 1998. Taxonomical response of the phytoplankton community of Upper Lake Constance (Bodensee-Obersee) to eutrophication and re-oligotrophication. In: Bäuerle, E., Gaedke, U. (Eds.), Lake Constance – Characterization of an Ecosystem in Transition, pp. 109–117.
Larrasoaña, J., Liu, Q., Hu, P., Roberts, A., Mata, P., Civis, J., Sierro, F., Pérez-Asensio, J., 2014. Paleomagnetic and paleoenvironmental implications of magnetofossil occurrences in late Miocene marine sediments from the Guadalquivir Basin, SW Spain. Front. Microbiol. 5 (71).
Larrasoaña, J.C., Roberts, A.P., Stoner, J.S., Richter, C., Wehausen, R., 2003. A new proxy for bottom-water ventilation in the eastern Mediterranean based on diagenetically controlled magnetic properties of sapropel-bearing sediments. Palaeogeogr. Palaeoclimatol. Palaeoecol. 190, 221–242.
Lehn, H., 1976. Veränderungen im Sauerstoffhaushalt des Bodensees. In: Müller, P. (Ed.), Verhandlungen der Gesellschaft für Ökologie Wien 1975: 5. Jahresversammlung vom 22. bis 24. September 1975 in Wien. Springer Netherlands, Dordrecht.
Lin, W., Paterson, G.A., Zhu, Q., Wang, Y., Kopylova, E., Li, Y., Knight, R., Bazylinski, D.A., Zhu, R., Kirschvink, J.L., Pan, Y., 2017. Origin of microbial biomineralization and magnetotaxis during the Archean. Proc. Natl. Acad. Sci. USA 114 (9), 2171–2176.
Maloof, A.C., Kopp, R.E., Grotzinger, J.P., Fike, D.A., Bosak, T., Vali, H., Poussart, P.M., Weiss, B.P., Kirschvink, J.L., 2007. Sedimentary iron cycling and the origin and preservation of magnetization in platform carbonate muds, Andros Island, Bahamas. Earth Planet. Sci. Lett. 259 (3), 581–598.
Meads, R.E., Malden, P.J., 1975. Electron spin resonance in natural kaolinites containing Fe3+ and other transition metal ions. Clay Miner. 10 (5), 313–345.
Melton, E.D., Stief, P., Behrens, S., Kappler, A., Schmidt, C., 2014. High spatial resolution of distribution and interconnections between Fe- and N-redox processes in profundal lake sediments. Environ. Microbiol. 16 (10), 3287–3303.
Muckle, R., 1967. Die Sauerstoffschichtung im tiefen Hypolimnion des Bodensee-Obersees 1963/64 mit Berücksichtigung einiger Untersuchungsergebnisse aus früheren Jahren. IGKB 3, 20.
Müller, G., 1966a. Die Verteilung von Eisenmonosulfid ($FeS.nH_2O$) und organischer Substanz in den Bodensedimenten des Bodensees – ein Beitrag zur Frage der Eutrophierung des Bodensees. Gas Wasserfach 107 (14), 364–368.
Müller, G., 1966b. Die Sedimentbildung im Bodensee. Naturwissenschaften 53 (10), 237–247.
Müller, G., 1997. Chronologie des anthropogenen Phosphor-Eintrags in den Bodensee und seine Auswirkung auf das Sedimentationsgeschehen. In: Matschullat, J., Tobschall, H.-J., Voigt, H.-J. (Eds.), Geochemie und Umwelt: Relevante Prozesse in Atmo-, Pedo- und Hydrosphäre. Springer, Berlin, Heidelberg, pp. 317–342.
Passier, H.F., de Lange, G.J., Dekkers, M.J., 2001. Magnetic properties and geochemistry of the active oxidation front and the youngest sapropel in the eastern Mediterranean Sea. Geophys. J. Int. 145 (3), 604–614.
Pike, C.R., Roberts, A.P., Verosub, K.L., 1999. Characterizing interactions in fine magnetic particle systems using first order reversal curves. J. Appl. Phys. 85 (9), 6660–6667.
Rahalkar, M., Deutzmann, J., Schink, B., Bussmann, I., 2009. Abundance and activity of methanotrophic bacteria in littoral and profundal sediments of Lake Constance (Germany). Appl. Environ. Microbiol. 75 (1), 119.
Rhodes, J., Hetzenauer, H., Frassl, M.A., Rothhaupt, K.-O., Rinke, K., 2017. Long-term development of hypolimnetic oxygen depletion rates in the large Lake Constance. Ambio 46 (5), 554–565.
Roberts, A.P., Florindo, F., Villa, G., Chang, L., Jovane, L., Bohaty, S.M., Larrasoaña, J.C., Heslop, D., Fitz Gerald, J.D., 2011. Magnetotactic bacterial abundance in pelagic marine environments is limited by organic carbon flux and availability of dissolved iron. Earth Planet. Sci. Lett. 310 (3), 441–452.
Roberts, A.P., Chang, L., Heslop, D., Florindo, F., Larrasoaña, J.C., 2012. Searching for single domain magnetite in the "pseudo-single-domain" sedimentary haystack: implications of biogenic magnetite preservation for sediment magnetism and relative paleointensity determinations. J. Geophys. Res., Solid Earth 117 (B8).
Roßknecht, H., 1998. Langjährige Entwicklung chemischer Parameter im Bodensee-Obersee. IGKB 48, 143.
Savian, J.F., Jovane, L., Frontalini, F., Trindade, R.I.F., Coccioni, R., Bohaty, S.M., Wilson, P.A., Florindo, F., Roberts, A.P., Catanzariti, R., Iacoviello, F., 2014. Enhanced primary productivity and magnetotactic bacterial production in response to middle Eocene warming in the Neo-Tethys Ocean. Palaeogeogr. Palaeoclimatol. Palaeoecol. 414, 32–45.
Scheffel, A., Gruska, M., Faivre, D., Linaroudis, A., Plitzko, J.M., Schüler, D., 2006. An acidic protein aligns magnetosomes along a filamentous structure in magnetotactic bacteria. Nature 440, 110.
Snowball, I.F., 1994. Bacterial magnetite and the magnetic properties of sediments in a Swedish lake. Earth Planet. Sci. Lett. 126 (1), 129–142.
Spormann, A.M., Wolfe, R.S., 1984. Chemotactic, magnetotactic and tactile behaviour in a magnetic spirillum. FEMS Microbiol. Lett. 22 (3), 171–177.
Spring, S., Schulze, R., Overmann, J., Schleifer, K.-H., 2000. Identification and characterization of ecologically significant prokaryotes in the sediment of freshwater lakes: molecular and cultivation studies. FEMS Microbiol. Rev. 24 (5), 573–590.
Suk, D., 2016. Environmental conditions for the presence of magnetofossils in the Last Glacial Maximum inferred from magnetic parameters of sediments from the Ulleung Basin, East Sea. Mar. Geol. 372, 53–65.
Vonsovskii, S.V., 1966. Magnetic resonance in ferromagnetics. In: Vonsovskii, S.V. (Ed.), Ferromagnetic Resonance: The Phenomenon of Resonant Absorption of a High-Frequency Magnetic Field in Ferromagnetic Substances. Pergamon, pp. 1–11.
Wagner, G., 1967. Beiträge zum Sauerstoff-, Stickstoff- und Phosphorhaushalt des Bodensees. Arch. Hydrobiol. 63 (1), 86–103.
Wagner, G., 1971. FeS-Konkretionen im Bodensee. Int. Rev. Gesamten Hydrobiol. Hydrograph. 56 (2), 265–272.
Wagner, G., Kruse, H.J., 1995. Analysis of the near-bottom oxygen minimum in Upper Lake Constance via statistical approach. Limnologica 25 (1), 11–20.
Wessels, M., 1995. Bodensee-Sedimente als Abbild von Umweltänderungen im Spät- und Postglazial. Gött. Arb. Geol. Paläontol. 66, 105.
Wessels, M., 1998a. Geological history of the Lake Constance area. In: Bäuerle, E., Gaedke, U. (Eds.), Lake Constance – Characterization of an Ecosystem in Transition, pp. 1–12.
Wessels, M., 1998b. Natural environmental changes indicated by Late Glacial and Holocene sediments from Lake Constance, Germany. Palaeogeogr. Palaeoclimatol. Palaeoecol. 140 (1), 421–432.
Wessels, M., Mohaupt, K., Kümmerlin, R., Lenhard, A., 1999. Reconstructing past eutrophication trends from diatoms and biogenic silica in the sediment and the pelagic zone of Lake Constance, Germany. J. Paleolimnol. 21 (2), 171–192.
Winklhofer, M., Zimanyi, G.T., 2006. Extracting the intrinsic switching field distribution in perpendicular media: a comparative analysis. J. Appl. Phys. 99 (8), 08E710.